Supporting Information

O'Gorman10.1073/pnas.1011547107

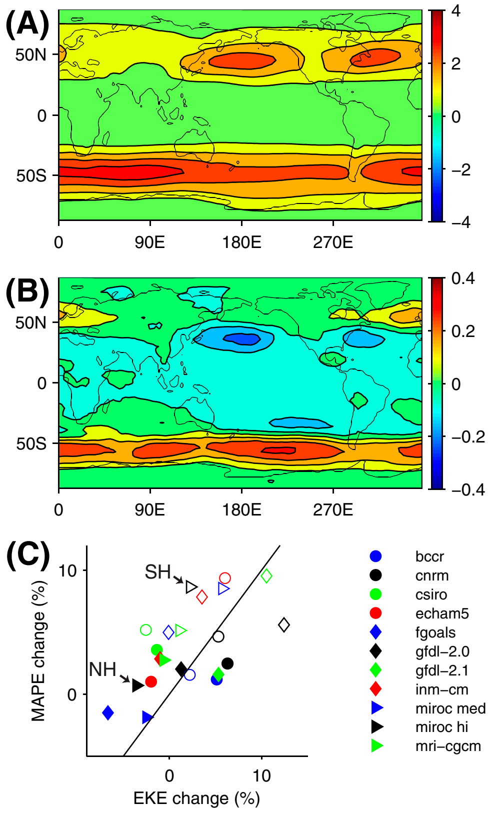

Fig. S1. Eddy kinetic energy (EKE) and mean available potential energy (MAPE) and their changes, as in Fig. 1, but for the annual average. The response of the storm tracks in each hemisphere is a combination of a change in intensity and a poleward shift.

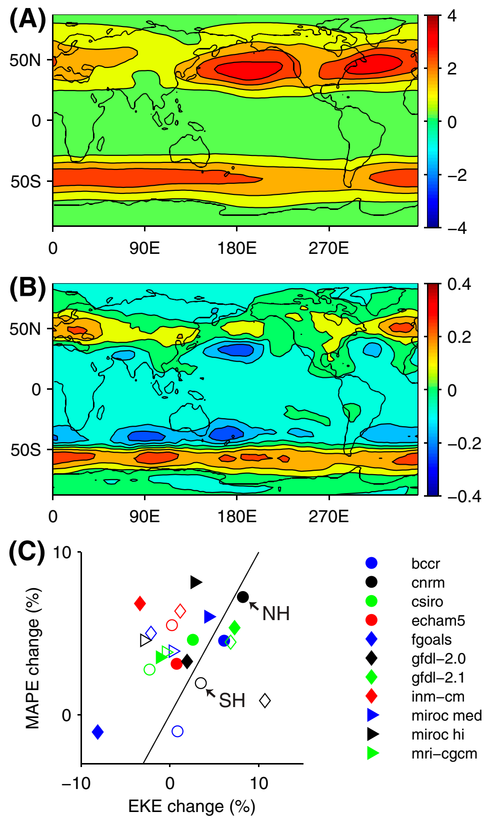

Fig. S2. Eddy kinetic energy (EKE) and mean available potential energy (MAPE) and their changes; as in Fig. 1, but for boreal winter (December-January-February). Unlike for boreal summer, there is a pronounced poleward shift of the storm tracks in both hemispheres, and smaller overall changes in both EKE and MAPE.

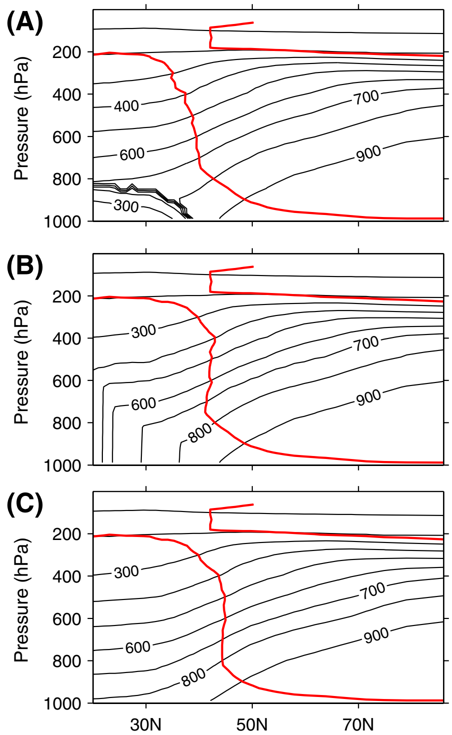

Fig. S3. Adiabatic rearrangements of air in the calculation of three types of mean available potential energy (MAPE) for June-July-August in the National Centers for Environmental Prediction–Department of Energy reanalysis. (*A*) Full MAPE. (*B*) Nonconvective MAPE. (*C*) Dry MAPE. The reference (minimum-enthalpy state) pressure (hPa) of air parcels is plotted as a function of latitude and pressure. The red line shows where the reference pressure equals the actual pressure, corresponding to no vertical movement of air parcels. For the full MAPE calculation, there is a discontinuity in the reference pressure at the edge of the subtropics; this discontinuity corresponds to the release of convective instability and the ascent of boundary-layer air to the upper troposphere.

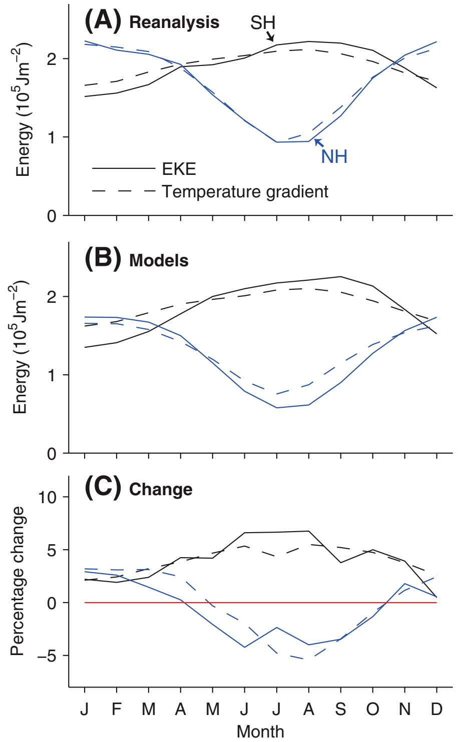

Fig. S4. As in Fig. 2, but using the meridional gradient of the zonal- and time- mean temperature at 500 hPa (dashed) rather than mean available potential energy. Results are shown for the southern hemisphere (black) and northern hemisphere (blue). The temperature gradient has been averaged with area weighting over the extratropics with a cutoff latitude of 20°. For *A* and *B*, it was then rescaled by a dimensional constant determined by a least-squares fit to the corresponding eddy kinetic energy (EKE) curve.

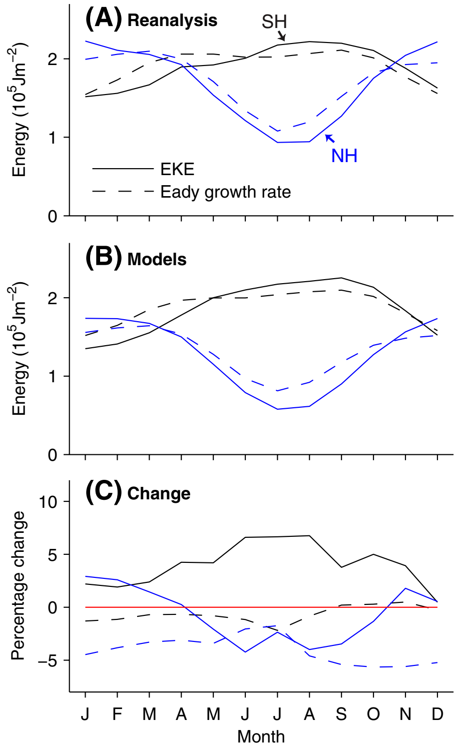

Fig. S5. As in Fig. 2, but using the maximum Eady growth rate for baroclinic instability (dashed) rather than mean available potential energy. There is approximate linear scaling between eddy kinetic energy (EKE) and the Eady growth rate over the seasonal cycle in a given climate (*A* and *B*), but not for climate change (*C*). The Eady growth rate was evaluated at 850 hPa using the zonal- and time-mean temperature and then averaged with area weighting over the extratropics with a cutoff latitude of 20°. For *A* and *B*, it was then rescaled by a dimensional constant determined by a least-squares fit to the corresponding EKE curve. Evaluation of the growth rate at 500 hPa does not improve the agreement.

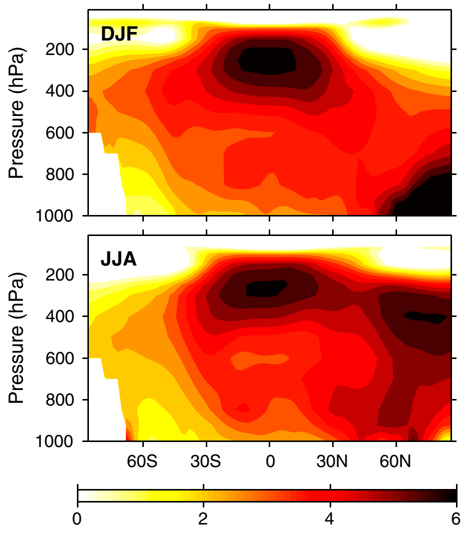

Fig. S6. Temperature changes (in kelvin) in December-January-February (DJF) and June-July-August (JJA); as in Fig. 3, but for the Model for Interdisciplinary Research on Climate (MIROC) medium resolution simulation. The MIROC simulations display strong Arctic warming, and have the largest decrease in northern hemisphere storm-track intensity in JJA of the simulations considered here. The same color contouring is used as in Fig. 3 to facilitate comparison, but note that the contouring is regionally saturated in this figure.

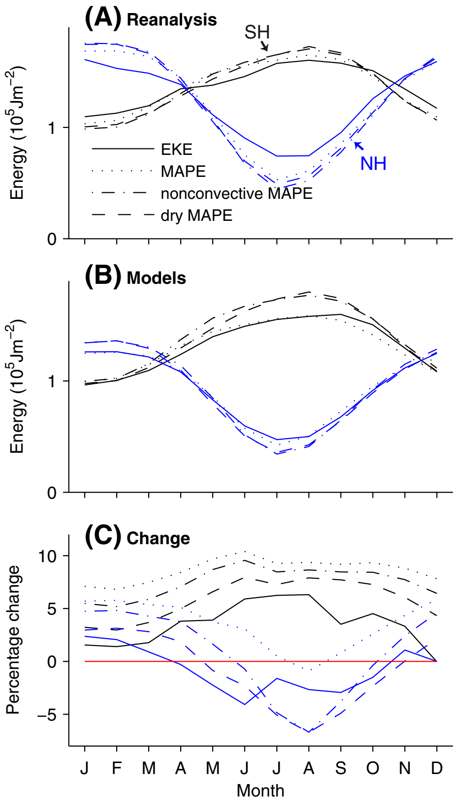

Fig. S7. Eddy kinetic energy and mean available potential energy (MAPE) and their changes; as in Fig. 2, but for the entire northern and southern hemispheres (rather than excluding latitudes equatorward of 20° latitude in each hemisphere). The effect of including the moist deep tropics is evident in the greater difference in behavior of dry and full MAPE.

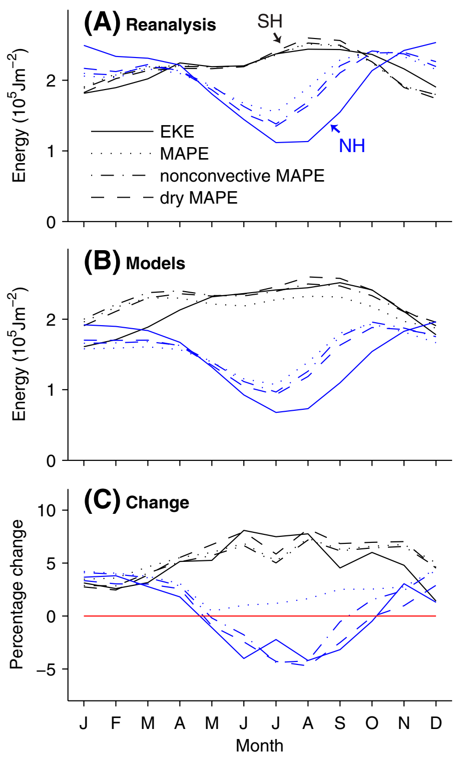

Fig. S8. Eddy kinetic energy and mean available potential energy (MAPE) and their changes; as in Fig. 2, but excluding latitudes below 30° latitude in each hemisphere (rather than 20°). The difference between fractional changes in full MAPE and nonconvective MAPE in northern hemispheric summer is particularly evident in *C*.

Table S1. Values of mean available potential energy (MAPE) (10^5 J m^{-2}) in the National Centers for Environmental Prediction–Department of Energy (NCEP-DOE) reanalysis and in the multimodel mean

		DJF		JJA		ANN	
	MAPE	SH	NH	SH	NH	SH	NH
NCEP-DOE	Full	34.0	36.7	42.2	20.8	36.9	29.6
	Nonconvective	32.2	36.6	41.9	17.6	36.2	28.9
	Dry	26.1	30.6	35.3	15.0	29.5	23.5
Models	Full	38.3	38.6	45.4	22.1	41.5	32.1
	Nonconvective	36.8	38.4	45.0	19.9	40.7	31.5
	Dry	28.7	32.7	37.7	15.9	32.8	25.5

Results are for the southern (SH) and northern (NH) hemispheres, excluding latitudes equatorward of 20° in each hemisphere. Values for three different types of MAPE are given: full MAPE, nonconvective MAPE, and dry MAPE. The calculations are based on temperatures and relative humidities that have been zonal- and time-averaged (1981–2000) for the seasons December-January-February (DJF), June-July-August (JJA), and over the whole time period (ANN).

Table S2. As in Table S1, but for mean available potential energy (MAPE) (10^5 J m^{-2}) calculated over entire hemispheres and not excluding the tropics

		DJF		JJA		ANN	
	MAPE	SH	NH	SH	NH	SH	NH
NCEP-DOE	Full	37.1	53.7	56.0	20.2	45.8	37.3
	Nonconvective	33.1	51.7	53.7	16.2	42.5	34.2
	Dry	27.4	41.6	43.5	14.1	34.3	27.5
Models	Full	42.4	57.8	63.8	23.1	52.9	41.9
	Nonconvective	38.1	55.7	61.1	19.0	49.5	39.0
	Dry	30.3	45.2	49.1	15.6	39.1	30.8

SH, southern hemisphere; NH, northern hemisphere; DJF, December-January-February; JJA, June-July-August; ANN, over the whole time period; NCEP-DOE, National Centers for Environmental Prediction–Department of Energy.